

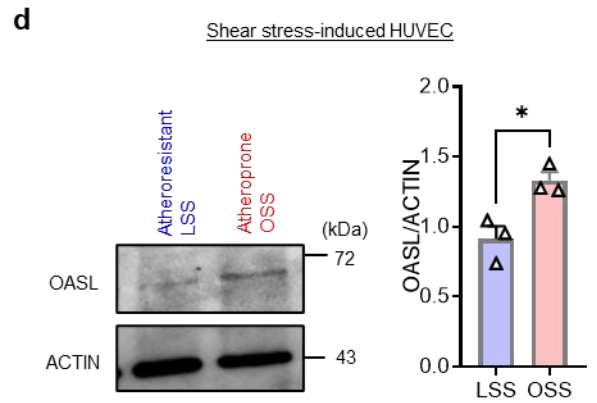
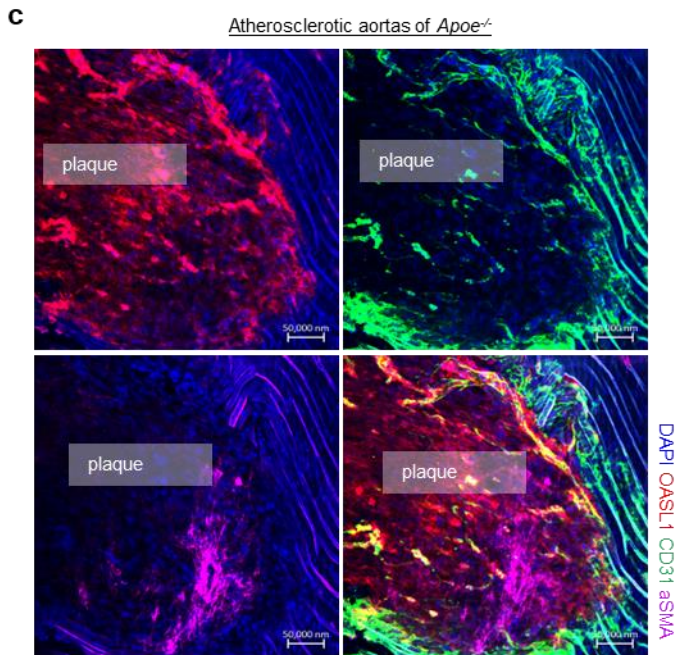
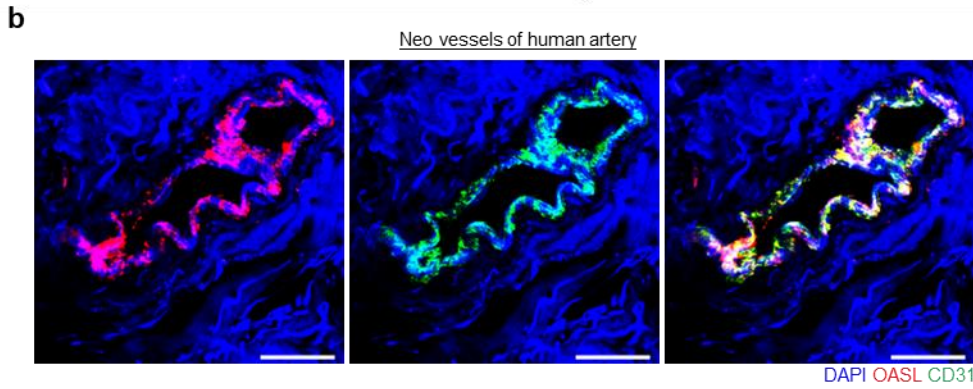
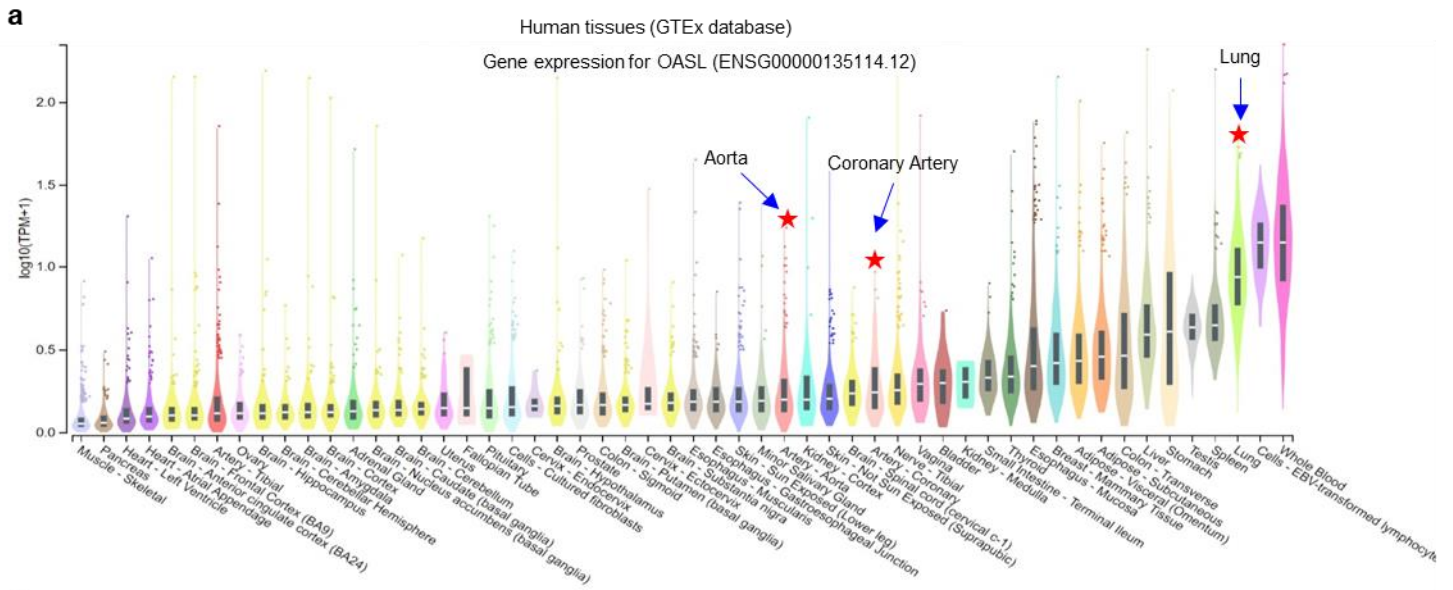
Supplementary Information

2'-5' Oligoadenylate Synthetase-Like 1 (OASL1) Protects Against Atherosclerosis by Maintaining Endothelial Nitric Oxide Synthase mRNA Stability

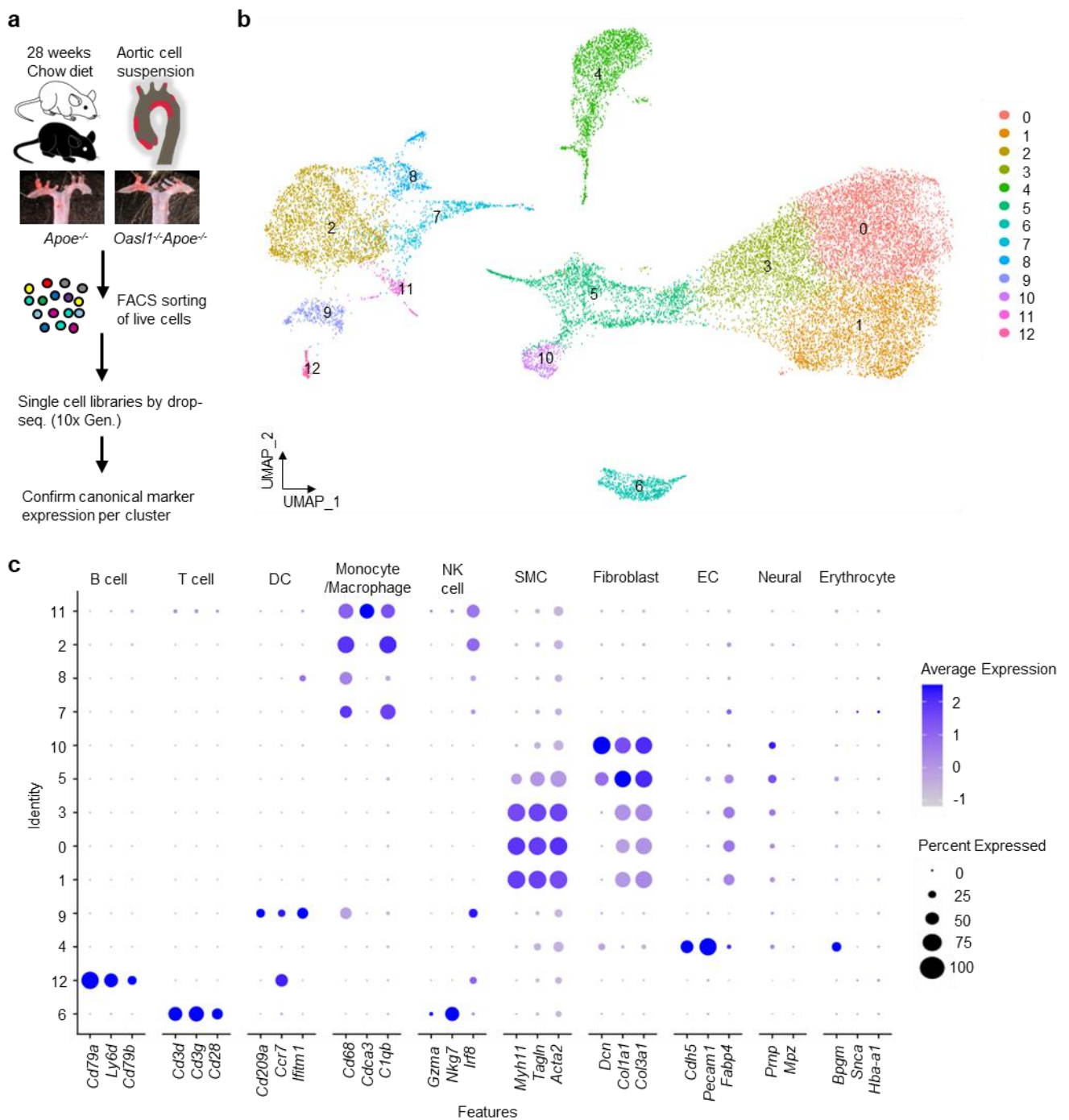
Tae Kyeong Kim et al.

Supplementary Figures 1–19

Supplementary Table 1

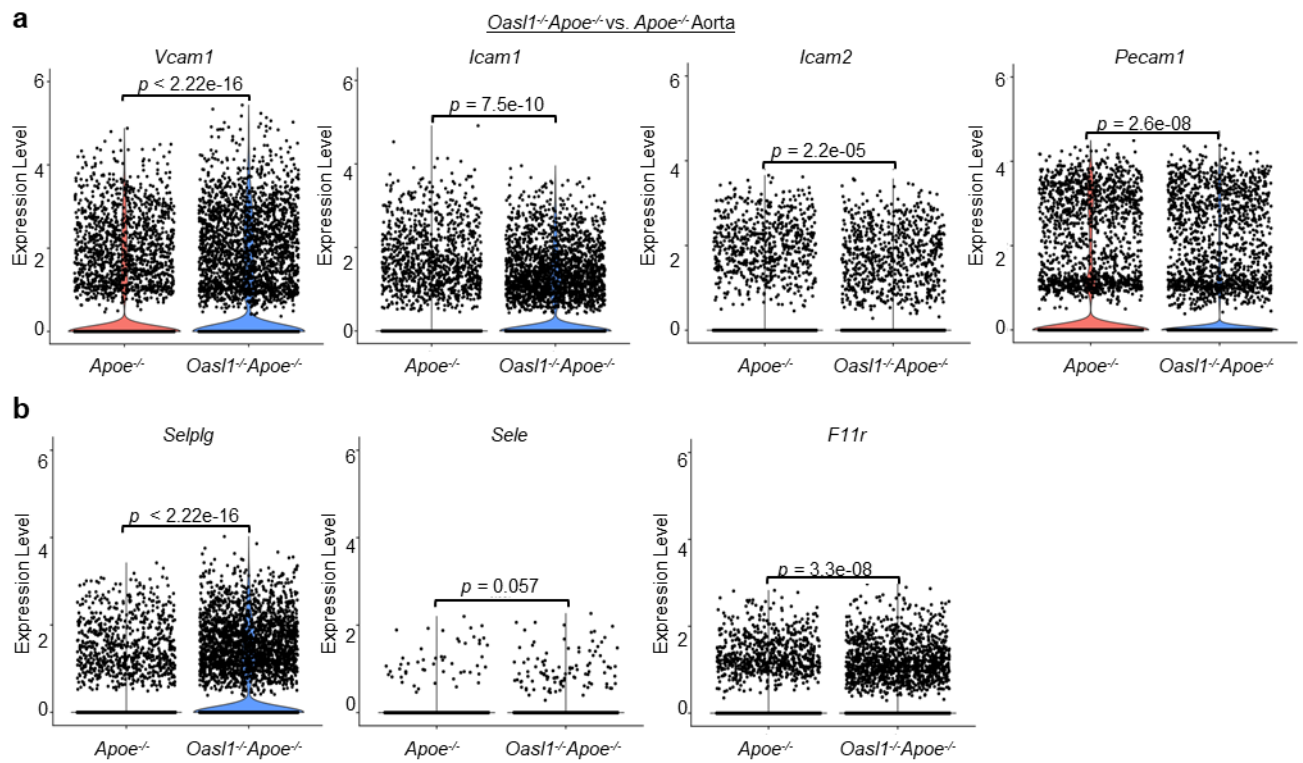


Supplementary Figure 1. Human OASL and murine OASL1 are expressed in vascular endothelial cells. **a** Mining of the GTEx database (<https://www.gtexportal.org/home/>) for RNA-sequencing data on OASL expression in normal human tissues. EC-enriched tissues, including coronary artery (sample size = 240, Median: 0.7513), lung (sample size = 578, Median: 7.679), and aorta (sample size = 432, Median: 0.5658) are highlighted and indicated. TPM, transcripts per million kilobases. Data were retrieved on Sep 06, 2022 (Data Source: GTEx Analysis Release V8 (dbGaP Accession phs000424.v8.p2)). Box plots are shown as median and 25th and 75th percentiles; points are displayed as outliers if they are above or below 1.5 times the interquartile range. **b** Immunofluorescence (IF) staining of OASL protein and CD31⁺ ECs in human atheroma tissues with plaques. Scale bars, 50 μ m. **c** *En face* IF staining for OASL1 and CD31⁺ ECs and α -SMA⁺ SMCs in plaque-containing *ApoE*^{-/-} aortas. Scale bars, 50 μ m. **d** Western blot analysis of OASL expression in shear-induced HUVECs ($p = 0.0189$, $n = 3$ per group). LSS: laminar shear stress. OSS: oscillatory shear stress. Data in **b** and **c** are representative of 3 independent experiments. Data are presented as means \pm SEMs ($*p \leq 0.05$; **d**, two-sided unpaired Student's *t*-test). Source data are provided as a Source Data file.

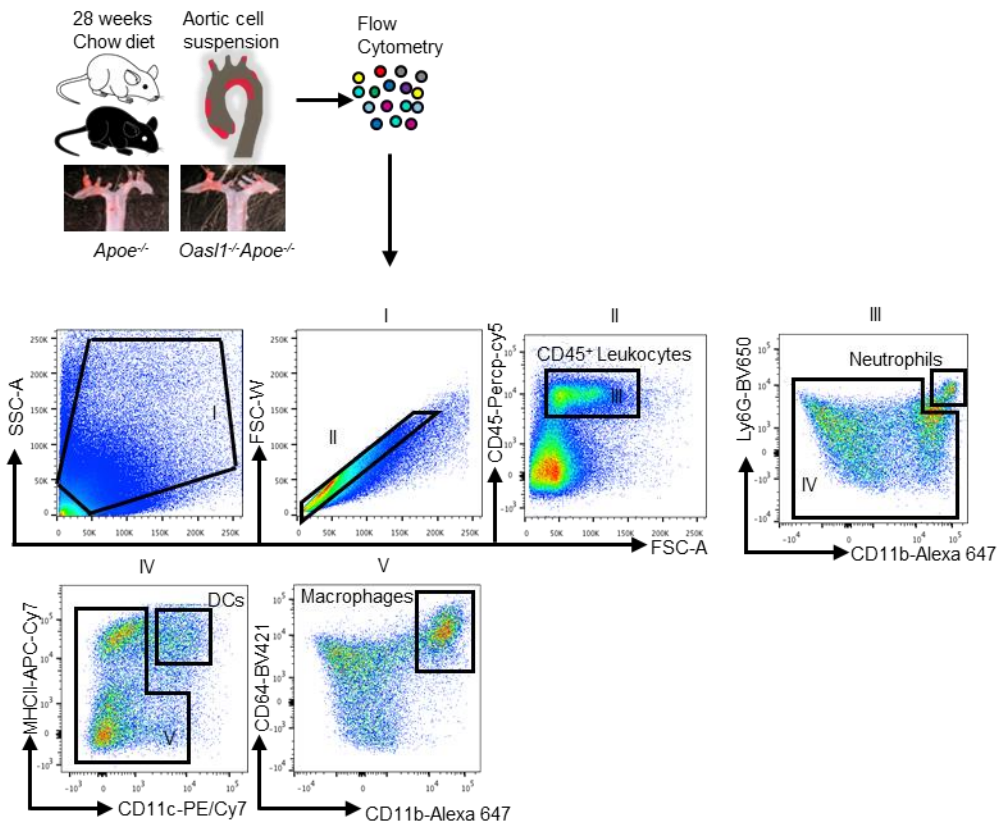


Supplementary Figure 2. scRNA-seq clustering of diverse cell populations from atherosclerotic aortas. a–c *Oasl1^{-/-}Apoe^{-/-}* and *Apoe^{-/-}* mice were maintained on a normal chow diet (NCD) for 28 weeks to allow the development of atherosclerotic plaques. **(a)** Experimental strategy for scRNA-seq of atherosclerotic aortic single cells. **(b)** Uniform manifold approximation and projection (UMAP) plot

of total aortic cells, colored by the numbering of clusters. (c) Dot plot represents the top markers in each aortic cell population. Dot size denotes the proportion of cells within the group expressing each transcript and dot color indicates the average expression level. DC: dendritic cell. NK cell: natural killer cell. SMC: smooth muscle cell. EC: endothelial cell.

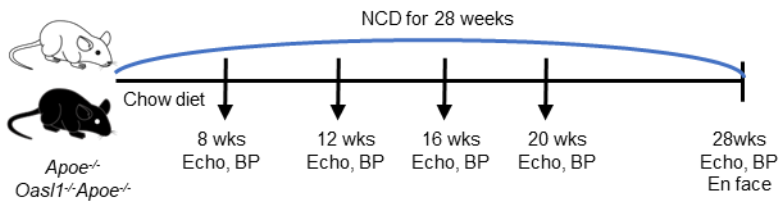
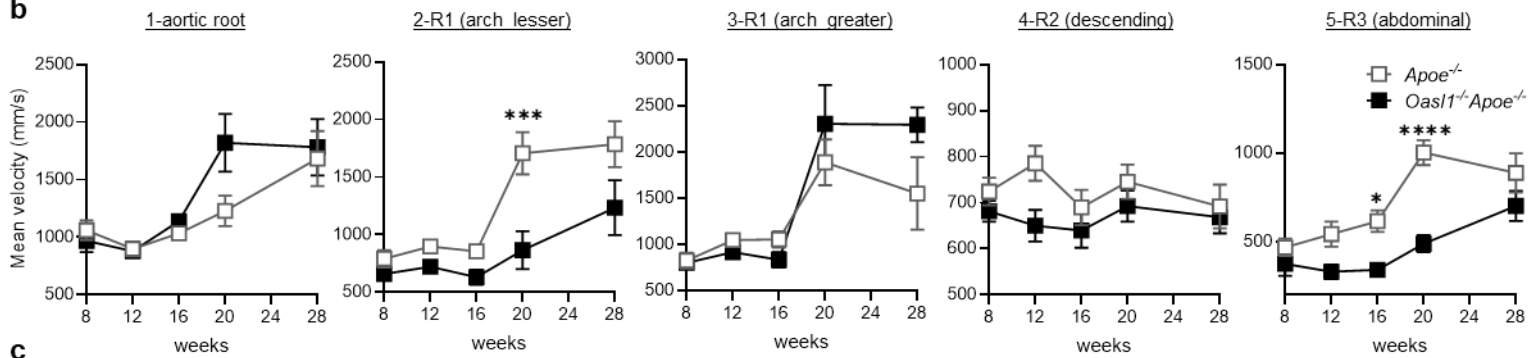
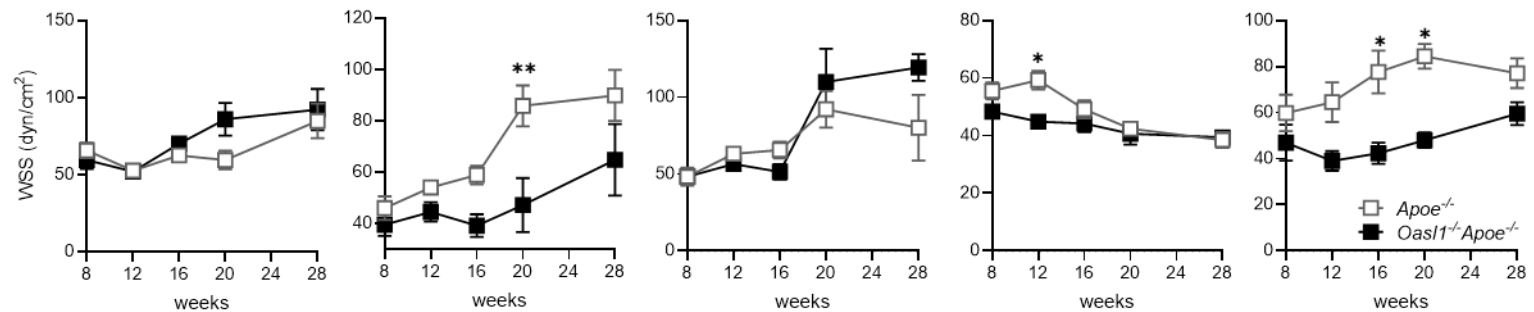


Supplementary Figure 3. *Oasl1* deficiency promotes proinflammatory gene expression in atherosclerotic aortas. a, b Violin plots showing the comparison of adhesion molecule expression in whole aortas. **(a)** *Vcam1*, *Icam1*, *Icam2*, and *Pecam1* expression. **(b)** *Selplg*, *Sele*, and *F11r* expression. Data are presented as means \pm SEMs (**a** and **b**, two-sided unpaired Student's *t*-test).



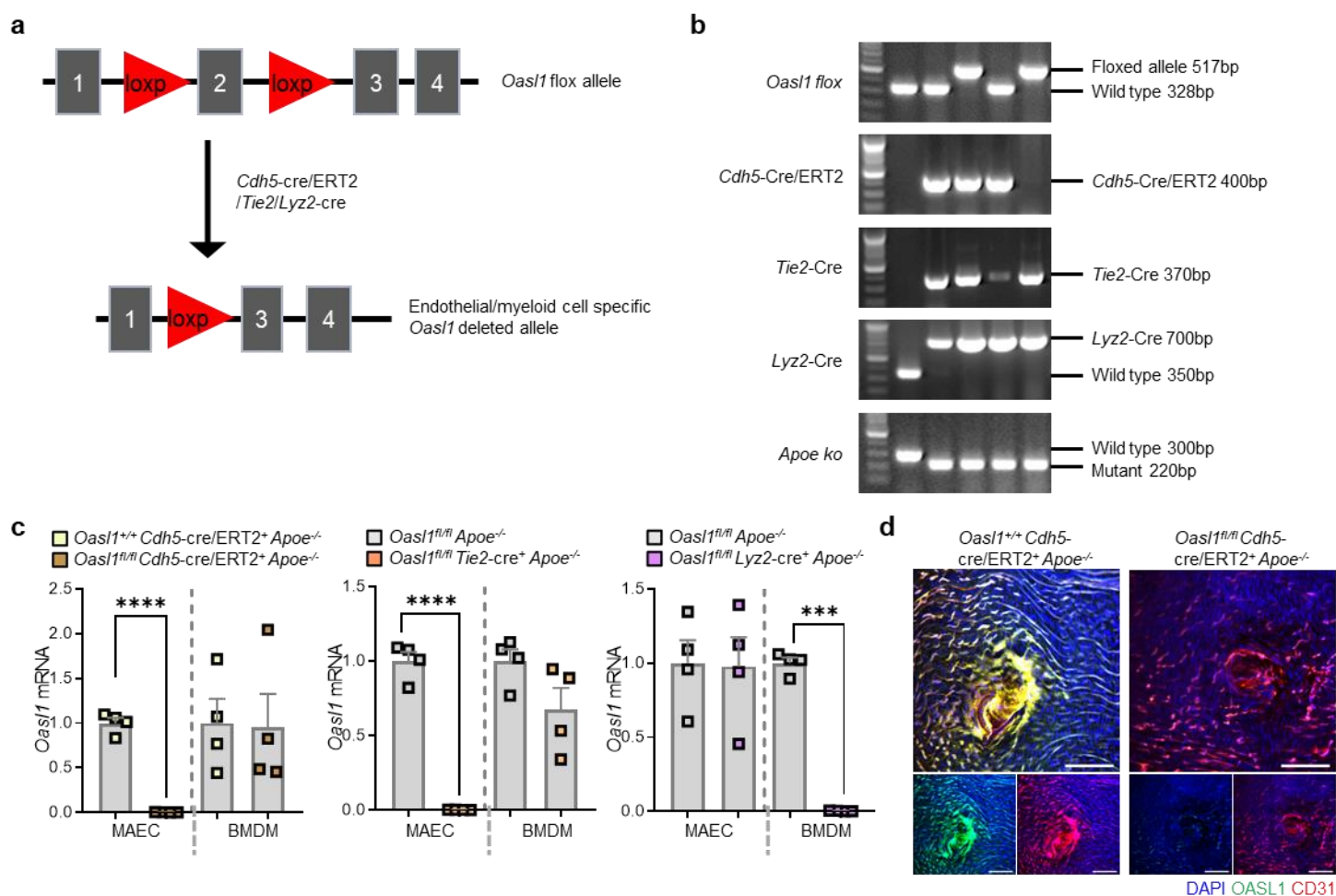
Supplementary Figure 4. Gating strategy for infiltrating immune cells in atherosclerotic aortas.

Oasl1^{-/-}*ApoE*^{-/-} and *ApoE*^{-/-} mice were maintained on a normal chow diet (NCD) for 28 weeks to allow for the development of atherosclerotic plaques. Experimental and gating strategy for flow cytometry analysis of atherosclerotic aortic single cells isolated from the *Oasl1*^{-/-}*ApoE*^{-/-} and *ApoE*^{-/-} mice.

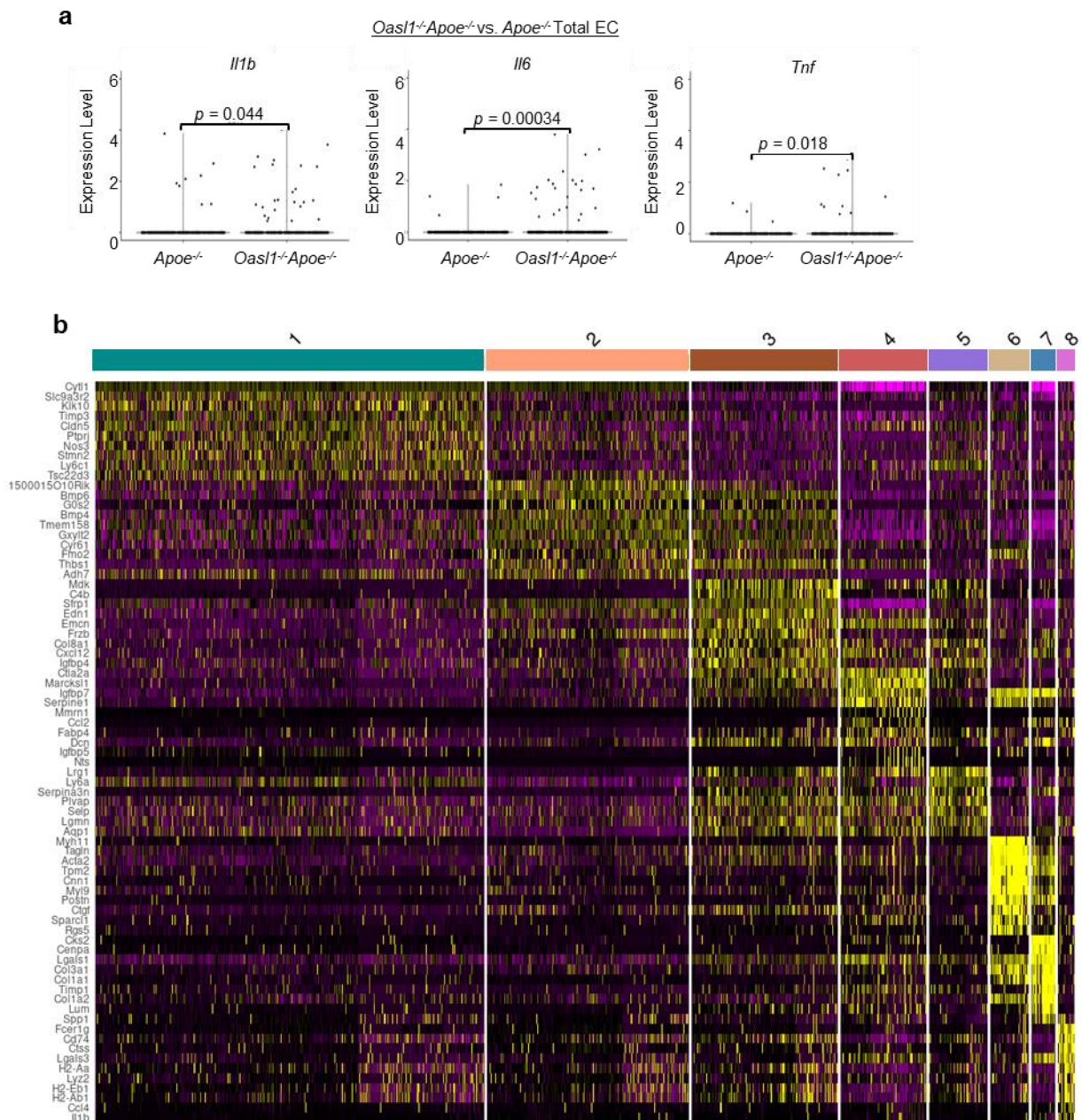
a**b****c**

Supplementary Figure 5. *Oas1* deficiency promotes endothelial dysfunction followed by a reduction of WSS under hyperlipidemic conditions. a–c Before identifying plaque formation at 28 weeks of NCD, the blood flow dynamics were assessed by serial echocardiography in age-matched *Oas1*^{-/-}*Apoe*^{-/-} and *Apoe*^{-/-} mice (n = 8 for 8–16; n = 6 for 20; n = 5 for 28 weeks per group). (a) Left: Experimental scheme. Right: Specific location of the ultrasound measurement in the *en face* of the aorta.

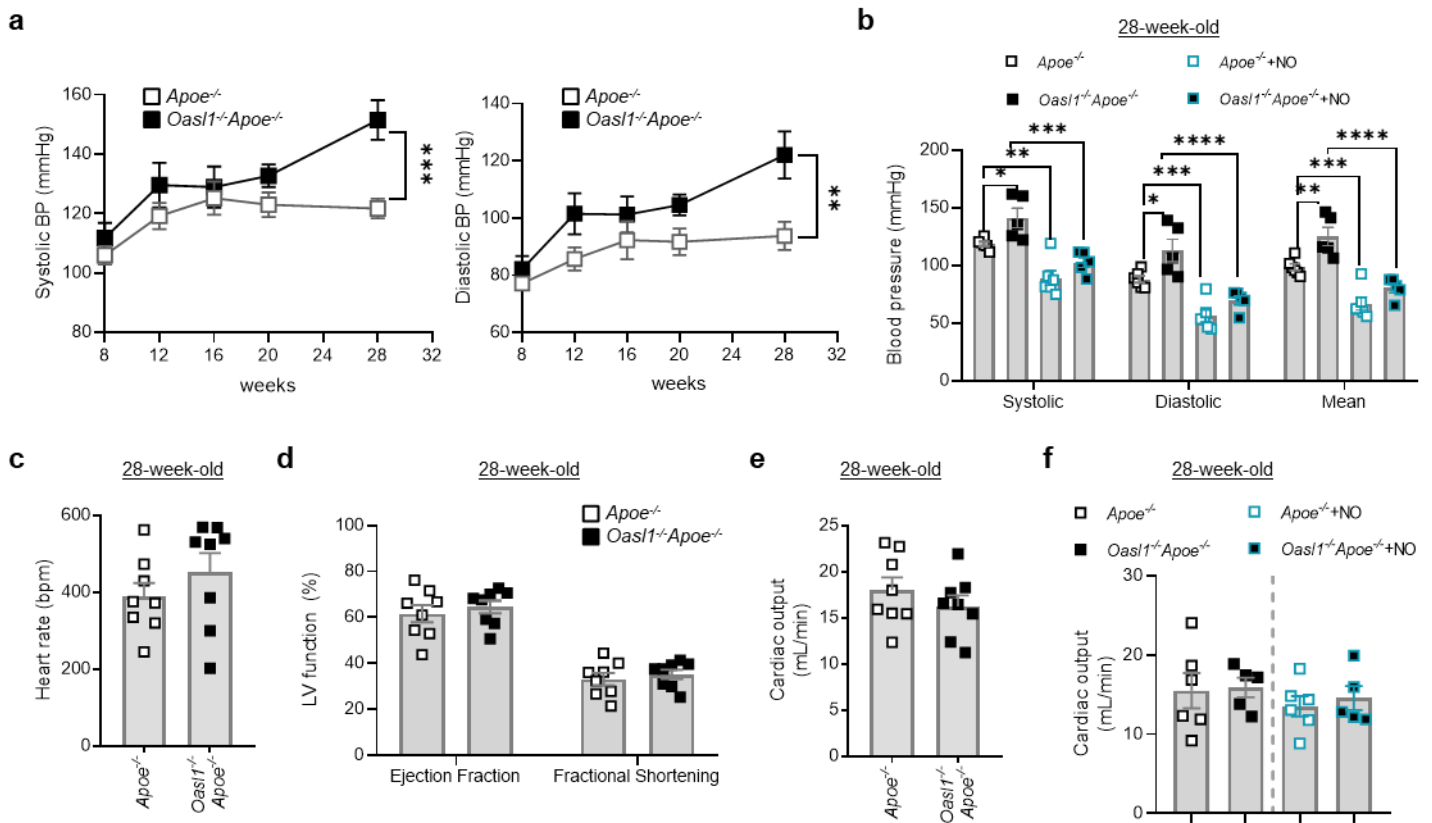
Mean blood velocity (R1 (lesser): $p = 0.0002$, R3: $p = 0.0444$; $p < 0.0001$) (**b**) and endothelial WSS (R1 (lesser): $p = 0.0050$, R3: $p = 0.0118$; $p = 0.0370$) (**c**) at the athero-resistant greater curvature or descending region and athero-prone lesser curvature or abdominal branching point were measured. BP: blood pressure. WSS: wall shear stress. Data are presented as means \pm SEMs ($*p \leq 0.05$, $**p \leq 0.01$, $***p \leq 0.001$, $****p \leq 0.0001$; **b–c**, two-way ANOVA with Tukey's test for multiple comparisons). Source data are provided as a Source Data file.



Supplementary Figure 6. Generation and characterization of endothelial cell-specific *Oasl1*-deficient mice. **a** Scheme for generating cell-specific *Oasl1* knockout mice using the Cre/LoxP system. **b** Genotyping of cell-specific *Oasl1* knockout mice. Molecular weight information is provided. **c** Confirmation of the deletion for *Oasl1* in endothelial cells (ECs) and bone marrow-derived macrophages (BMDMs) isolated from each cre-expressing *Oasl1*^{fl/fl} mouse by qRT-PCR analysis (*Cdh5* cre MAEC: $p < 0.0001$, *Tie2* cre MAEC: $p < 0.0001$, *Lyz2* cre BMDM: $p < 0.0001$, $n = 4$ per group). *Oasl1* expression in the non-endothelial cell fraction was unaffected, indicating the specific knockout of *Oasl1* in ECs. **d** *En face* IF staining for OASL1 and CD31⁺ ECs in the endothelium of aortas isolated from *Oasl1*^{fl/fl} *Cdh5*-cre/ERT2⁺ *Apoe*^{-/-} and *Oasl1*^{+/+} *Cdh5*-cre/ERT2⁺ *Apoe*^{-/-} mice. Scale bar, 50 μ m. BMDM: bone marrow-derived macrophages. Data are presented as means \pm SEMs (** $p \leq 0.001$, **** $p \leq 0.0001$; **c**, two-sided unpaired Student's *t*-test). Source data are provided as a Source Data file.

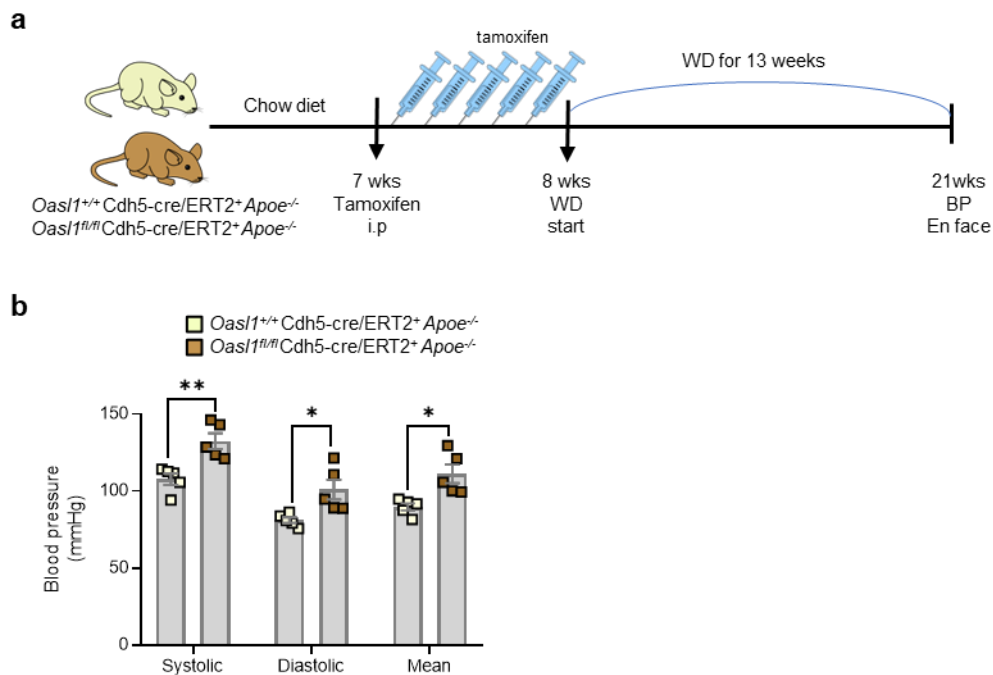


Supplementary Figure 7. *Oasl1*-deficient ECs exhibit inflammatory characteristics. **a** Violin plot comparing the expression of the inflammatory cytokines, *Il1b*, *Il6*, and *Tnf*, in the EC cluster of whole aortas isolated from *Oasl1^{-/-}Apoe^{-/-}* and *Apoe^{-/-}* mice. **b** Heat map representation showing different gene expression patterns among the EC sub-clusters. Data are presented as means \pm SEMs (**a**, two-sided unpaired Student's *t*-test).

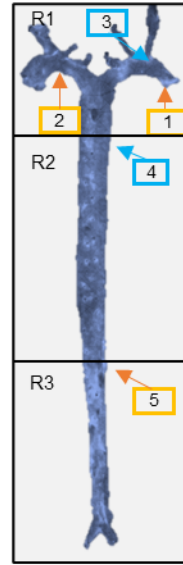
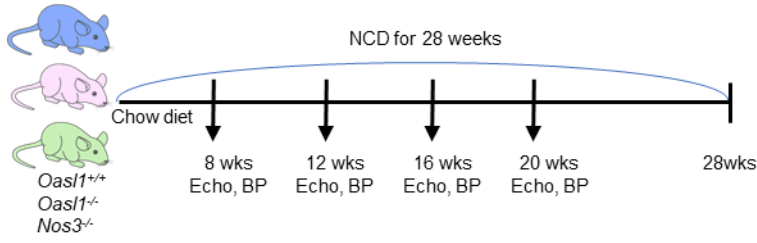
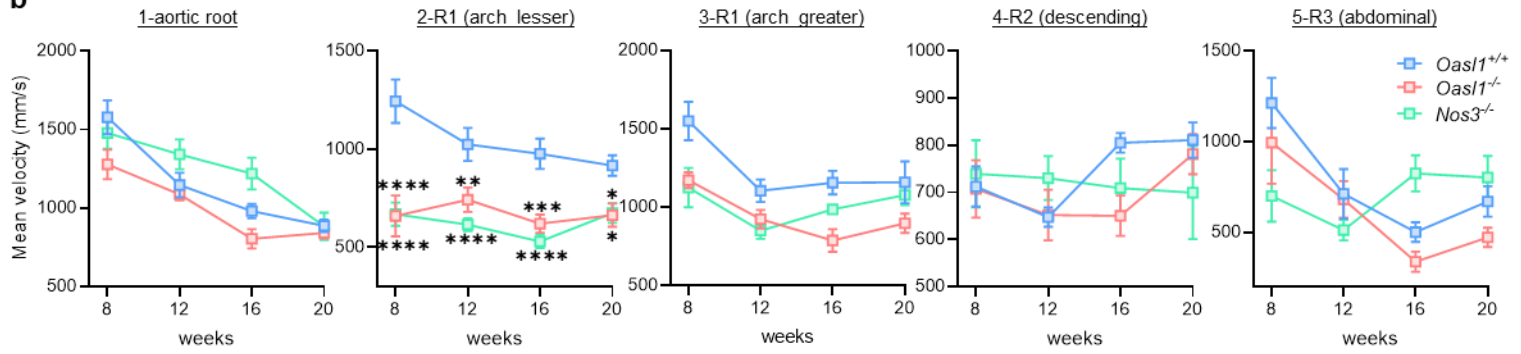
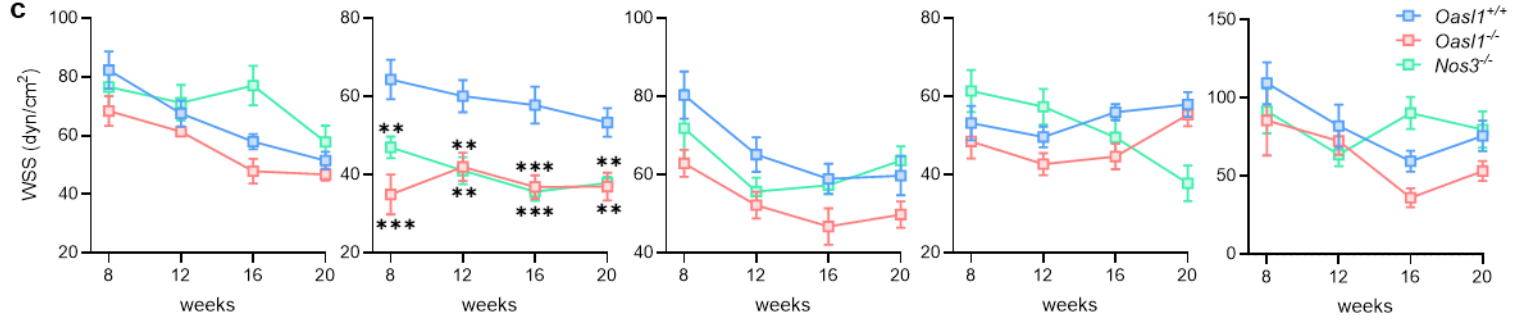
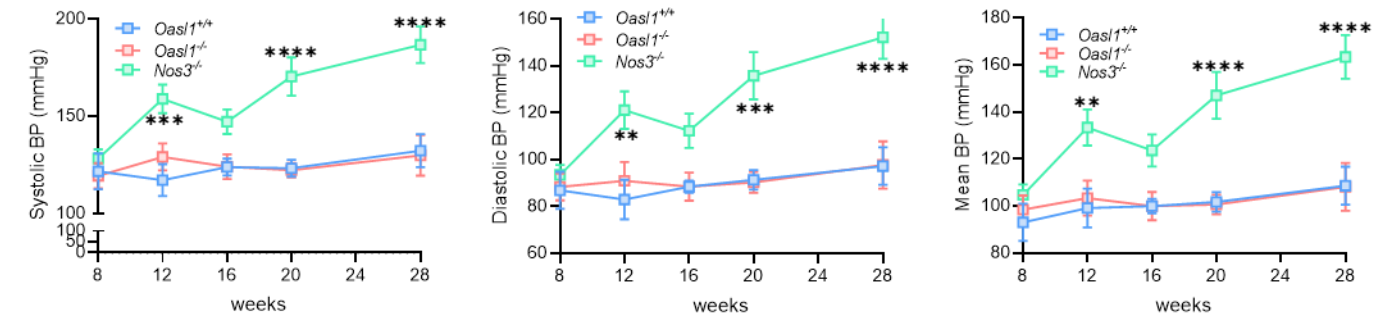


Supplementary Figure 8. *Oasl1* deficiency increases blood pressure dependent on NO levels without affecting cardiac function. a–f $Apoe^{-/-}$ and $Oasl1^{-/-}Apoe^{-/-}$ mice were fed an NCD for 28 weeks to allow for atherosclerotic conditions to develop. (a) Left: Systolic blood pressure (BP; $p = 0.0009$) and Right: diastolic BP ($p = 0.0030$) change measured using tail-cuff techniques ($n = 7$ per group). (b) BP measurement after nitric oxide (NO) supplementation by DETANONATE injection into 28-week-old mice (Systolic: $p = 0.0309$; $p = 0.0013$; $p = 0.0001$, Diastolic: $p = 0.0123$; $p = 0.0005$; $p < 0.0001$, Mean: $p = 0.0071$; $p = 0.0006$; $p < 0.0001$, $n = 6$ for $Apoe^{-/-}$, $Apoe^{-/-}+NO$; $n = 5$ for $Oasl1^{-/-}Apoe^{-/-}$, $Oasl1^{-/-}Apoe^{-/-}+NO$). c Heart rate measured using a tail-cuff system ($n = 8$ per group). d, e Left ventricle (LV) function was measured by serial echocardiography and calculated using Vevo software ($n = 8$ per group). (d) Ejection fraction and fractional shortening. (e) Cardiac output. f Cardiac output measurement after NO supplementation by DETANONATE injection into 28-week-old mice (n

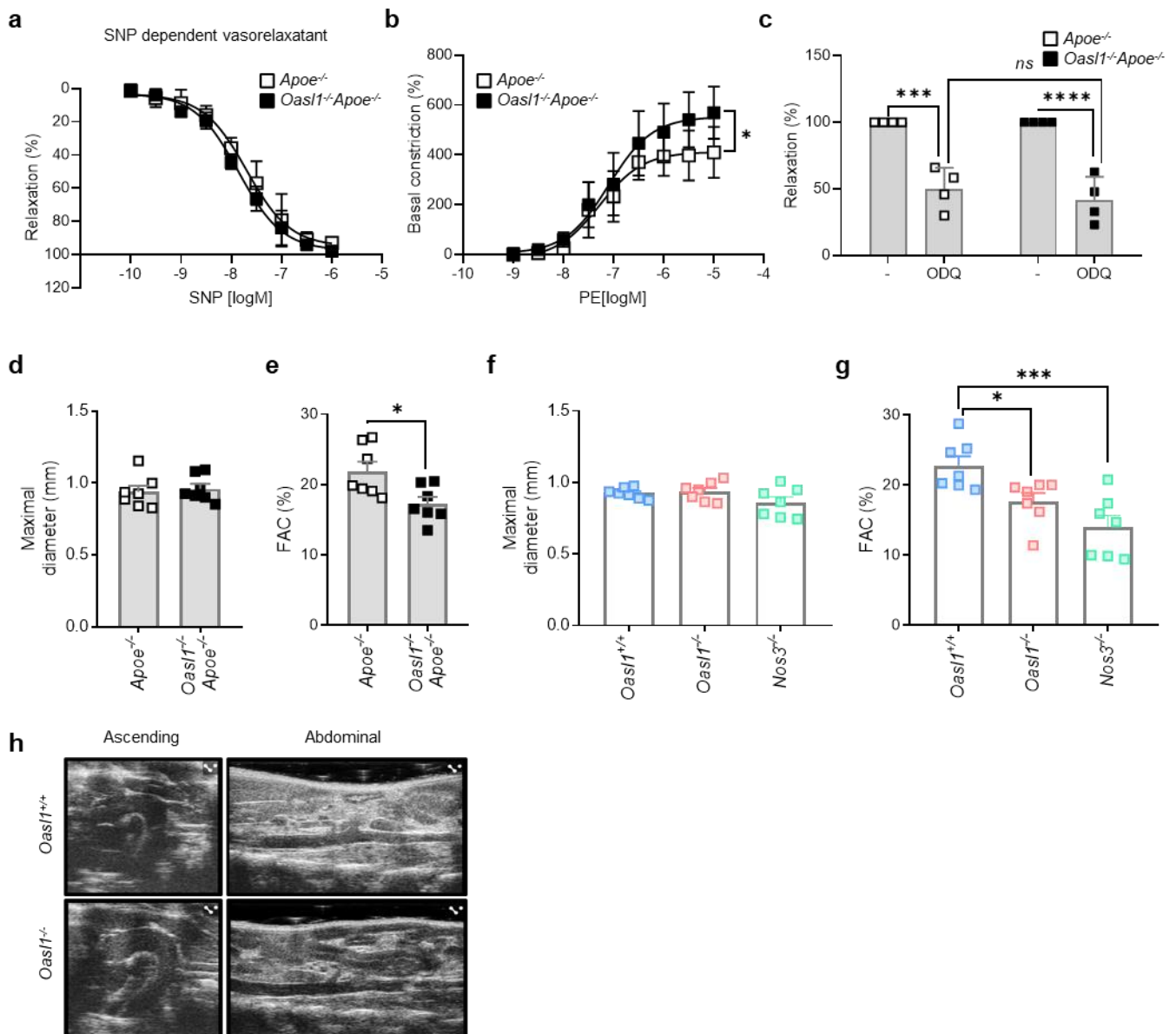
= 6 for *ApoE*^{-/-}, *ApoE*^{-/-}+NO; n = 5 for *Oasl1*^{-/-}*ApoE*^{-/-}, *Oasl1*^{-/-}*ApoE*^{-/-}+NO). Data are presented as means ± SEMs (**p* ≤ 0.05, ***p* ≤ 0.01, ****p* ≤ 0.001, *****p* ≤ 0.0001; **a**, two-way ANOVA with Sidak's test; **b** and **f**, two-way ANOVA with Tukey's test for multiple comparisons; **c–e**, two-sided unpaired Student's *t*-test). Source data are provided as a Source Data file.



Supplementary Figure 9. Endothelial *Oasl1* deficiency increases blood pressure following plaque formation. **a–b** Blood pressure (BP) was measured in age-matched *Oasl1*^{fl/fl} *Cdh5-cre/ERT2*⁺ *Apoe*^{-/-} and *Oasl1*^{+/+} *Cdh5-cre/ERT2*⁺ *Apoe*^{-/-} mice after being fed a western diet (WD) for 13 weeks. **(a)** Experimental scheme. **(b)** Systolic, diastolic, and mean BP change measured using tail-cuff techniques (Systolic: $p = 0.0044$, Diastolic: $p = 0.0188$, Mean: $p = 0.0106$, $n = 5$ per group). Data are presented as means \pm SEMs ($*p \leq 0.05$, $**p \leq 0.01$; **b**, two-sided unpaired Student's t -test). Source data are provided as a Source Data file.

a**b****c****d**

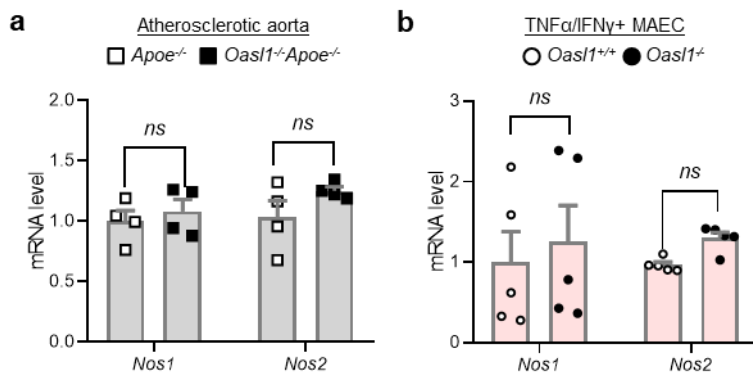
Supplementary Figure 10. *Oasl1* deficiency reduces blood velocity and WSS. a–d Blood pressure (BP) and blood flow dynamics were measured in age-matched *Oasl1*^{-/-}, *Nos3*^{-/-} and *Oasl1*^{+/+} mice. **(a)** Left: Experimental scheme. Right: Specific location for ultrasound measurement in the *en face* of the aorta. Mean blood velocity (R1 (lesser) 8: $p < 0.0001$; $p < 0.0001$, 12: $p = 0.0090$; $p < 0.0001$, 16: $p = 0.0007$; $p < 0.0001$, 20: $p = 0.0218$; $p = 0.0292$) **(b)** and endothelial WSS (R1 (lesser) 8: $p < 0.0001$; $p = 0.0030$, 12: $p = 0.0019$; $p = 0.0010$, 16: $p = 0.0003$; $p = 0.0001$, 20: $p = 0.0052$; $p = 0.0091$) **(c)** at the athero-resistant greater curvature or descending region and athero-prone lesser curvature or abdominal branching point as assessed by serial echocardiography (n = 8 per group except n = 5 for 8-week-old *Oasl1*^{-/-}). **(d)** Left: Systolic BP (*Nos3*^{-/-} vs. *Oasl1*^{+/+} 12: $p = 0.0004$, 20: $p < 0.0001$, 28: $p < 0.0001$), Middle: diastolic BP (*Nos3*^{-/-} vs. *Oasl1*^{+/+} 12: $p = 0.0011$, 20: $p = 0.0001$, 28: $p < 0.0001$) and Right: mean BP (*Nos3*^{-/-} vs. *Oasl1*^{+/+} 12: $p = 0.0034$, 20: $p < 0.0001$, 28: $p < 0.0001$) change measured using tail-cuff techniques (n = 7 per group). WSS: wall shear stress. Data are presented as means \pm SEMs (* $p \leq 0.05$, ** $p \leq 0.01$, *** $p \leq 0.001$, **** $p \leq 0.0001$; **b–d**, two-way ANOVA with Tukey’s test for multiple comparisons). Source data are provided as a Source Data file.



Supplementary Figure 11. *Oasl1* deficiency reduces vascular tension and increases constriction.

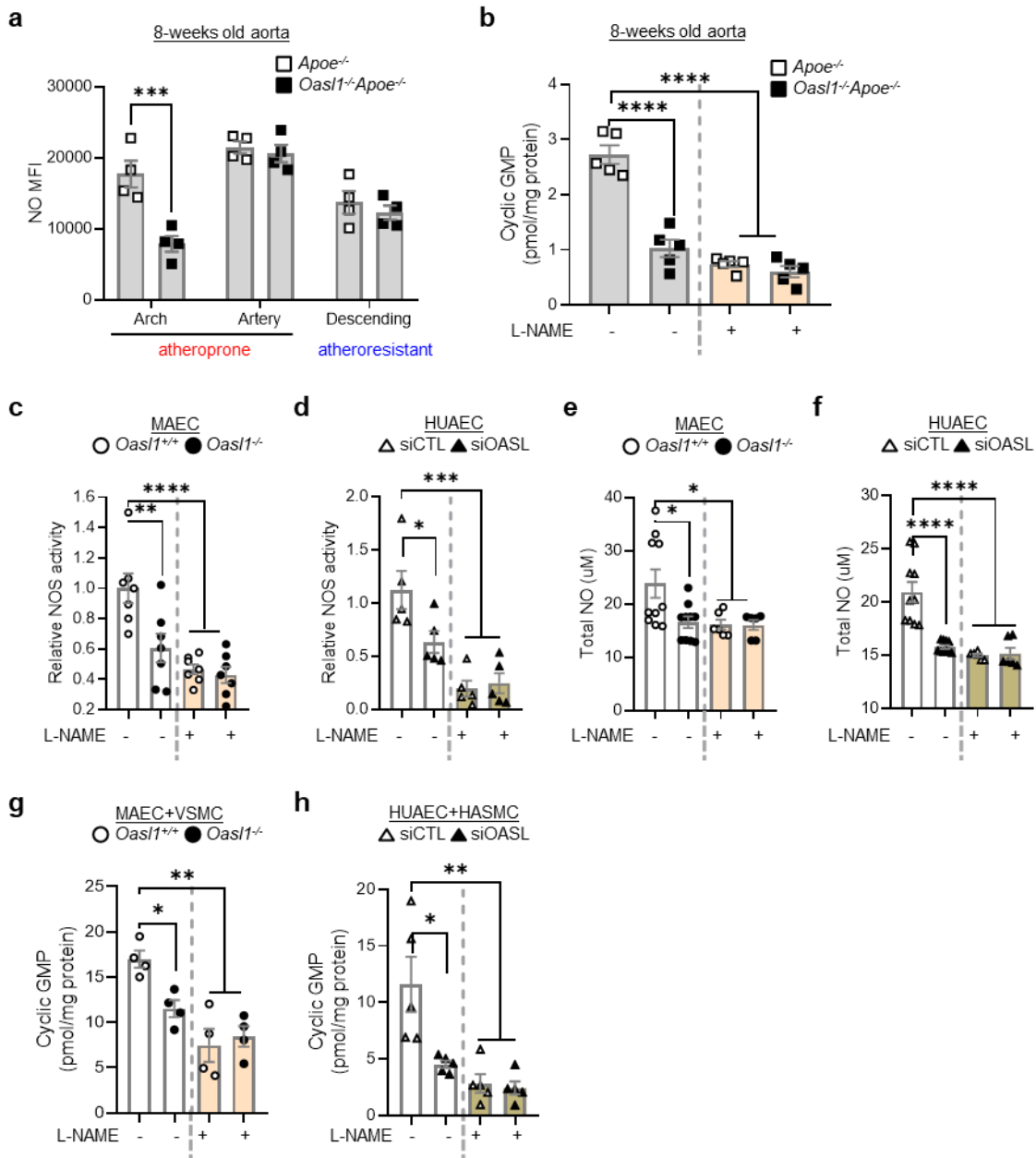
a–c The cumulative vascular response of the aortic rings isolated from *Oasl1*^{-/-}*Apoe*^{-/-} and *Apoe*^{-/-} mice as measured by myography (n = 4 per group). **(a)** Relaxation response to sodium nitroprusside (SNP). **(b)** Constriction response to phenylephrine (PE; *p* = 0.0109). **(c)** The percentage of relaxation response in 1H-[1,2,4]oxadiazolo[4,3-a]quinoxalin-1-one (ODQ) treatment compared with the control (*Apoe*^{-/-}: *p* = 0.0004, *Oasl1*^{-/-}*Apoe*^{-/-}: *p* < 0.0001, n = 4 per group). **d, e** *Apoe*^{-/-} and *Oasl1*^{-/-}*Apoe*^{-/-}

mice were fed an NCD for 16 to 20 weeks and subjected to ultrasound measurements (n = 7 per group). **(d)** Maximal diameter. **(e)** The percentage of fractional area change (FAC; $p = 0.0176$). **f–h** *Oasl1*^{-/-}, *Nos3*^{-/-} and *Oasl1*^{+/+} mice were fed an NCD for 16 to 20 weeks and subjected to ultrasound measurements. **(f)** Maximal diameter (n = 7 per group). **(g)** The percentage of FAC ($p = 0.0474$; $p = 0.0009$, n = 7 per group). **(h)** Vascular geometry. Data are presented as means \pm SEMs except **a–c**; means \pm SDs ($*p \leq 0.05$, $***p \leq 0.001$, $****p \leq 0.0001$; Nonlinear fit data in **a** and **b** were calculated using a Sigmoidal dose-response and two-sided unpaired Student's *t*-test; **c**, two-way ANOVA with Sidak's test; **d** and **e**, two-sided unpaired Student's *t*-test; **f** and **g**, one-way ANOVA with Tukey's test for multiple comparisons). Source data are provided as a Source Data file.



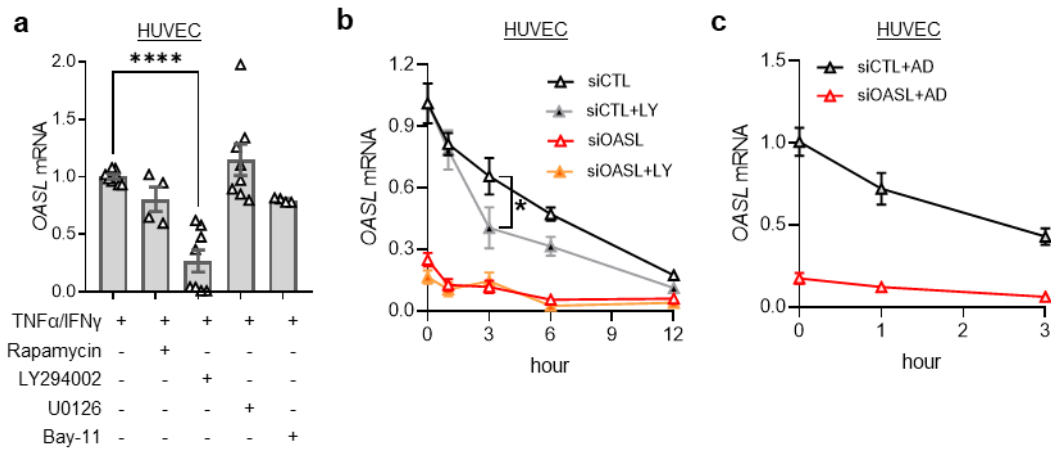
Supplementary Figure 12. *Oasl1* deficiency has little effect on the expression of other *Nos* genes.

Nos1 and *Nos2* expression was measured in atherosclerotic aortas (n = 4 per group) (a) or in MAECs stimulated with TNF α and IFN γ (n = 5 per group) (b) by quantitative PCR analysis. Data are presented as means \pm SEMs (a and b, two-sided unpaired Student's t-test). Source data are provided as a Source Data file.

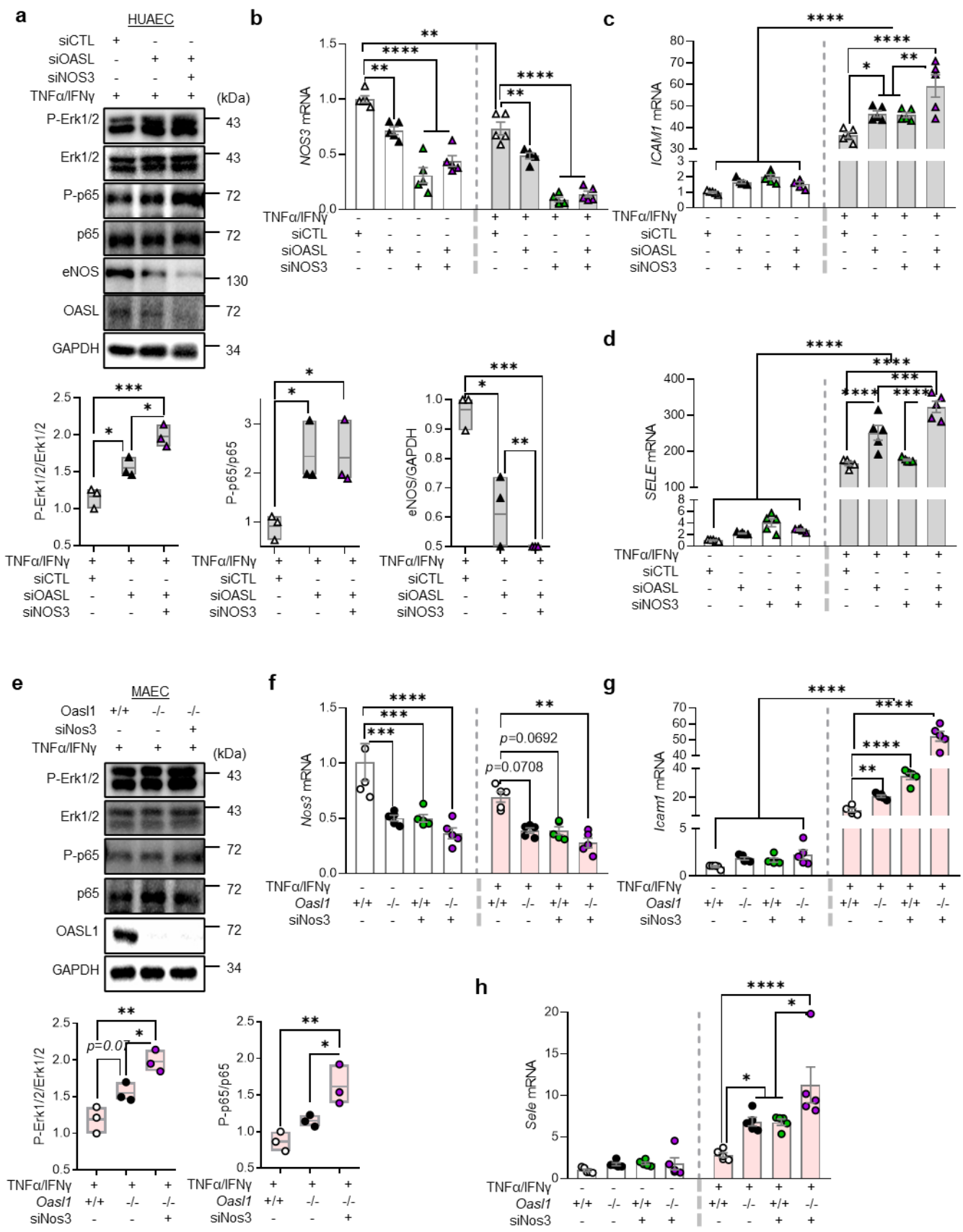


Supplementary Figure 13. *Oasl1* deficiency reduces eNOS/NO bioavailability followed by a decrease in aortic cGMP levels. a–b Aorta tissues were isolated from $Apoe^{-/-}$ and $Oasl1^{-/-}Apoe^{-/-}$ mice fed an NCD for 8 weeks. (a) Quantitation of nitric oxide (NO) MFI results according to regional specificity ($p = 0.0041$, $n = 4$ per group). (b) Cyclic guanosine monophosphate (cGMP) level in aortas following incubation with or without N^G -nitro-L-arginine methyl ester (L-NAME) for 24 h (vs.

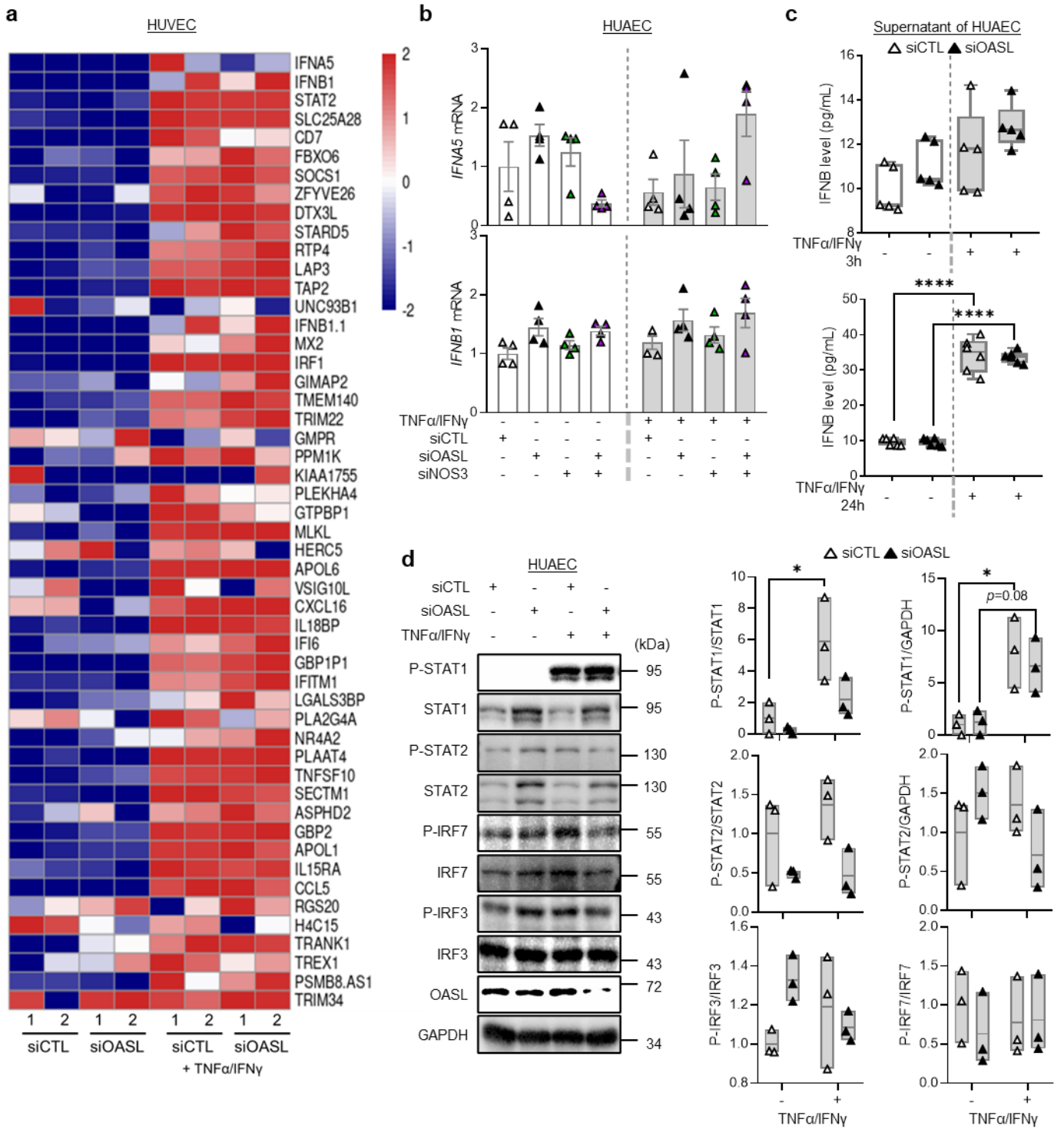
Apoe^{-/-} -L-NAME: $p < 0.0001$; $p < 0.0001$, $n = 5$ per group). Analysis of NOS enzymatic activity in MAECs isolated from *Oasl1*^{+/+} and *Oasl1*^{-/-} mice (vs. *Oasl1*^{+/+} -L-NAME: $p = 0.0018$; $p < 0.0001$; $p < 0.0001$, $n = 7$ per group) (c) and in HUAECs transfected with siCTL or siOASL (vs. siCTL -L-NAME: $p = 0.0379$; $p = 0.0003$; $p = 0.0006$, $n = 5$ per group) (d) following treatment with L-NAME. Total nitric oxide (NO) levels in the supernatants of ECs including MAECs isolated from *Oasl1*^{+/+} and *Oasl1*^{-/-} mice (vs. *Oasl1*^{+/+} -L-NAME: $p = 0.0239$; $p = 0.0416$; $p = 0.0396$, $n = 10$ for non-treat; $n = 6$ for L-NAME) (e) and HUAECs transfected with siCTL or siOASL (vs. siCTL -L-NAME: $p < 0.0001$; $p < 0.0001$; $p < 0.0001$, $n = 10$ for non-treat; $n = 6$ for L-NAME) (f) following treatment with L-NAME for 24 h. Cyclic GMP (cGMP) levels in mouse VSMCs co-cultured with MAECs (vs. *Oasl1*^{+/+} -L-NAME: $p = 0.0324$; $p = 0.0010$; $p = 0.0022$, $n = 4$ per group) (g) and human VSMCs co-cultured with HUAECs (vs. siCTL -L-NAME: $p = 0.0110$; $p = 0.0023$; $p = 0.0016$, $n = 5$ per group) (h) following incubation with or without L-NAME for 24 h. Data are presented as means \pm SEMs ($*p \leq 0.05$, $**p \leq 0.01$, $***p \leq 0.001$, $****p \leq 0.0001$; a, two-sided unpaired Student's t-test; b-d, g and h, two-way ANOVA with Tukey's test; e and f, one-way ANOVA with Tukey's test for multiple comparisons). Source data are provided as a Source Data file.



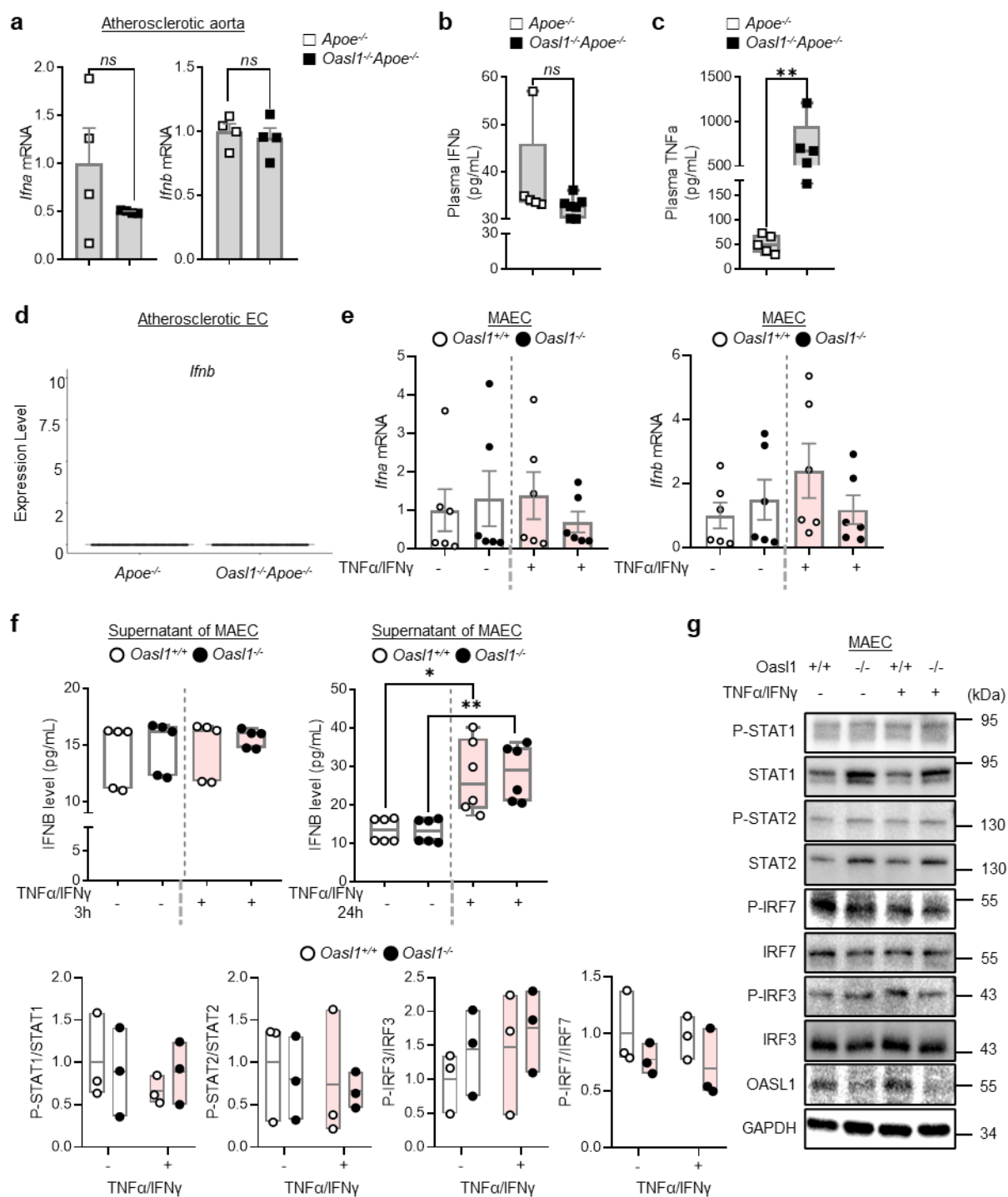
Supplementary Figure 14. *OASL* expression is suppressed by PI3K/Akt inhibition. qRT-PCR analysis of *OASL* mRNA in (a) HUVECs pretreated with the mTOR inhibitor, rapamycin, PI3K inhibitor, LY294002, MEK1/2 inhibitor, U0126, or NF- κ B inhibitor, Bay-11 (20 μ mol/L each) 1 h before stimulation with TNF- α and IFN- γ for 3 h ($p < 0.0001$, $n = 8$ for DMSO, LY294002, U0126; $n = 4$ for Rapamycin, Bay11), and (b) siCTL- or siOASL-transfected HUVECs, pretreated with the PI3K inhibitor, LY294002 (LY), and monitored over time (siCTL vs. siCTL+LY 3h: $p = 0.0096$, $n = 4$ per group). c Confirmation of *OASL* mRNA levels in siCTL- or siOASL-transfected HUVECs. *OASL* mRNA was measured over time in the presence of actinomycin D (AD), which was added to block transcription ($n = 4$ per group). Data are presented as means \pm SEMs ($*p \leq 0.05$, $****p \leq 0.0001$; a, one-way ANOVA with Bonferroni's test; b and c, two-way ANOVA with Tukey's test for multiple comparisons). Source data are provided as a Source Data file.



Supplementary Figure 15. *Nos3* knockdown potentiates endothelial inflammation in *Oasl1*-deficient ECs. **a–d** siCTL- or siOASL-transfected HUAECs were co-transfected with siNOS3 and stimulated with TNF- α and IFN- γ . **(a)** Top: Western blot analysis of Erk1/2, p65, and eNOS expression. Bottom: Quantitation of band density (P-Erk1/2: $p = 0.0315$; $p = 0.0009$; $p = 0.0217$, P-p65: $p = 0.0455$; $p = 0.0485$, eNOS: $p = 0.0181$; $p = 0.0003$; $p = 0.0065$). Quantitative PCR analysis of *NOS3* (non siOASL: $p = 0.0011$; siNOS3, siOASL/siNOS3: $p < 0.0001$, non vs. T/I siCTL: $p = 0.0026$, T/I siOASL: $p = 0.0063$; siNOS3, siOASL/siNOS3: $p < 0.0001$) **(b)** and the adhesion molecules *ICAM1* (non vs. T/I: $p < 0.0001$, T/I siOASL: $p = 0.0298$; siOASL/siNOS3: $p < 0.0001$; siOASL or siNOS3 vs. siOASL/siNOS3: $p = 0.0020$; $p = 0.0011$) **(c)** and *SELE* (non vs. T/I: $p < 0.0001$, T/I siOASL, siOASL/siNOS3: $p < 0.0001$; siOASL or siNOS3 vs. siOASL/siNOS3: $p = 0.0001$; $p < 0.0001$) **(d)** ($n = 5$ per group). **e–h** MAECs isolated from *Oasl1*^{+/+} and *Oasl1*^{-/-} mice were co-transfected with siNos3 and stimulated with TNF- α and IFN- γ . **(e)** Top: Western blot analysis of Erk1/2 and p65 expression. Bottom: Quantitation of band density (P-Erk1/2: $p = 0.0019$; $p = 0.0336$, P-p65: $p = 0.0054$; $p = 0.0438$). Quantitative PCR analysis of *Nos3* (non *Oasl1*^{-/-}, siNos3: $p = 0.0003$; *Oasl1*^{-/-}/siNos3: $p < 0.0001$, T/I *Oasl1*^{-/-}/siNos3: $p = 0.0042$) **(f)** and the adhesion molecules *Icam1* (non vs. T/I: $p < 0.0001$, T/I *Oasl1*^{-/-}: $p = 0.0010$; siNos3, *Oasl1*^{-/-}/siNos3: $p < 0.0001$) **(g)** and *Sele* (T/I *Oasl1*^{-/-}: $p = 0.0389$; siNos3: $p = 0.0455$, *Oasl1*^{-/-}/siNos3: $p < 0.0001$; *Oasl1*^{-/-} vs. *Oasl1*^{-/-}/siNos3: $p = 0.0174$; siNos3 vs. *Oasl1*^{-/-}/siNos3: $p = 0.0147$) **(h)** ($n = 5$ per group). Data in **a** and **e** are representative of 3 independent experiments. **a** and **e**, Box plots are shown as median of each value and the interquartile range (IQR, the range between the 25th and 75th percentiles). Data are presented as means \pm SEMs ($*p \leq 0.05$, $**p \leq 0.01$, $***p \leq 0.001$, $****p \leq 0.0001$; **a** and **e**, one-way ANOVA with Tukey's test; **b–d**, **f–h**, two-way ANOVA with Tukey's test for multiple comparisons). Source data are provided as a Source Data file.

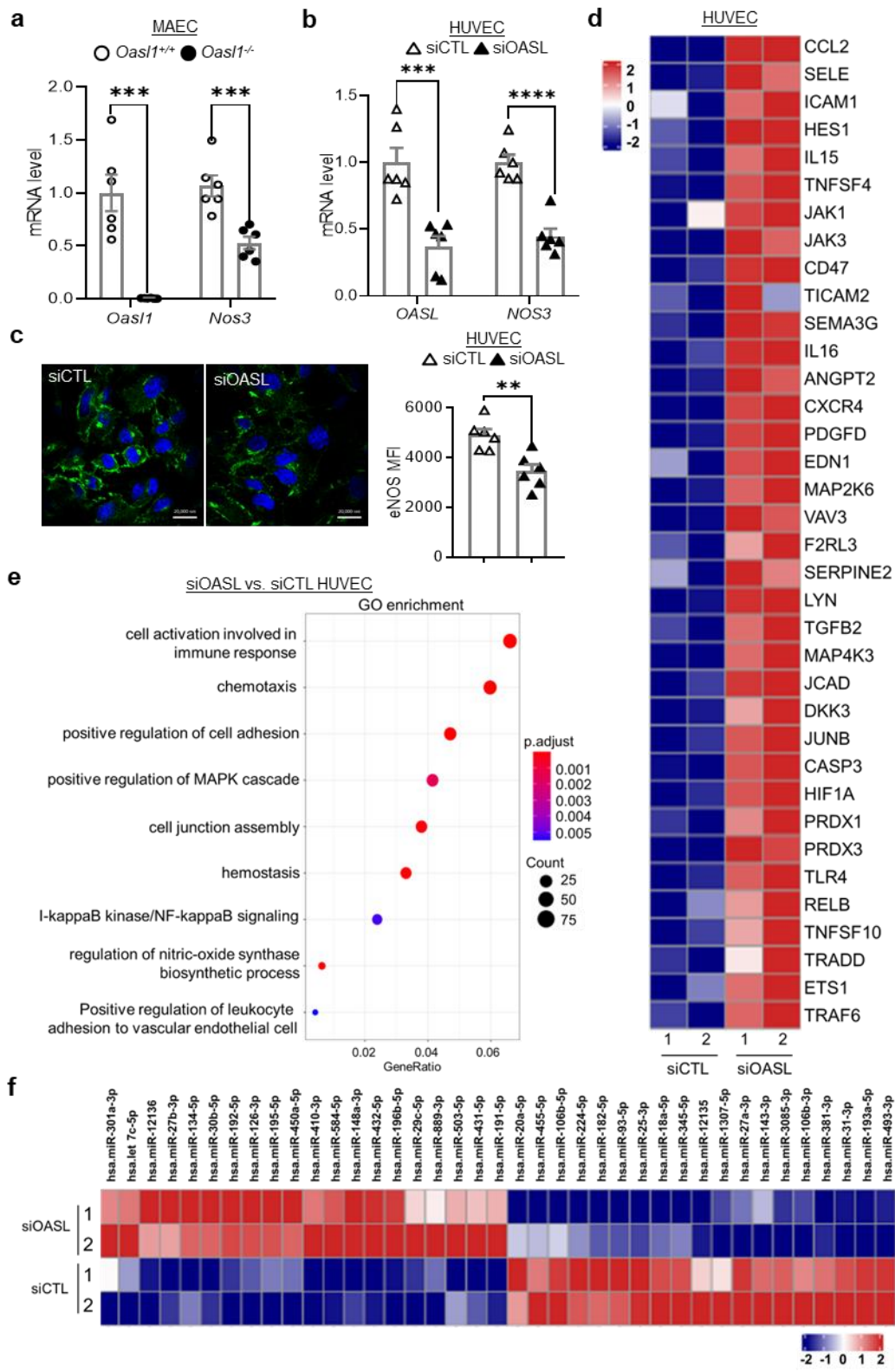


Supplementary Figure 16. Endothelial *OASL* knockdown shows no differences in type I IFN signaling. **a** Heatmap of type I interferon (IFN)-stimulated genes from bulk RNA-seq analysis performed on siCTL- or siOASL-transfected HUVECs stimulated with or without TNF α and IFN γ (n = 2 per group). **b** Quantitative PCR analysis of *IFNA5* and *IFNB1* in siCTL- or siOASL-transfected HUAECs co-transfected with siNOS3 and stimulated with TNF- α and IFN- γ (n = 4 per group). **c–d** siCTL- or siOASL-transfected HUVECs were stimulated with TNF- α and IFN- γ . (c) Secreted IFNB levels in the supernatants of HUAECs. Top: stimulated for 3 h (n = 5 per group). Bottom: stimulated for 24 h (siCTL: $p < 0.0001$, siOASL: $p < 0.0001$, n = 6 per group). (d) Left: Western blot analysis of STAT1, STAT2, IRF7, and IRF3 expression. Right: Quantification of band density (P-STAT1/STAT1: $p = 0.0305$, P-STAT1/GAPDH: $p = 0.0121$; $p = 0.0420$). **c** and **d**, Box plots are shown as median of each value and the IQR; whiskers indicate 1.5 times the IQR. Data in **d** are representative of 3 independent experiments. Data are presented as means \pm SEMs ($*p \leq 0.05$, $****p \leq 0.0001$; **b** and **c**, two-way ANOVA with Tukey's test; **d**, two-way ANOVA with Sidak's test for multiple comparisons). Source data are provided as a Source Data file.

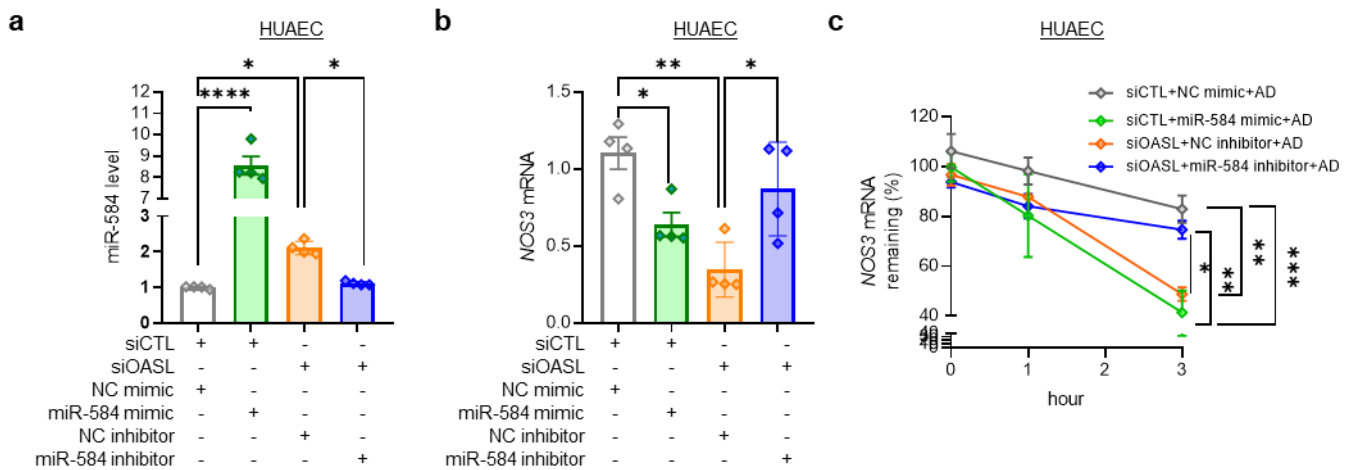


Supplementary Figure 17. Endothelial *Oas1* deficiency shows no differences in type I IFN signaling. a–d *Apoe*^{-/-} and *Oas1*^{-/-}*Apoe*^{-/-} mice were fed an NCD for 28 weeks to allow atherosclerotic conditions to develop. (a) Quantitative PCR analysis of type I IFNs, *Ifna* and *Ifnb*, in

atherosclerotic aortas (n = 4 per group). **(b)** Plasma IFN β levels. (n = 5 for *Apoe*^{-/-}; n = 7 for *Oasl1*^{-/-}*Apoe*^{-/-}) **(c)** Plasma TNF α levels. (*p* = 0.0066, n = 5 per group). **(d)** Violin plot comparing *Ifnb* in the aortic EC cluster of *Oasl1*^{-/-}*Apoe*^{-/-} versus *Apoe*^{-/-} mice. **e–g** MAECs isolated from *Oasl1*^{+/+} and *Oasl1*^{-/-} mice and stimulated with TNF α and IFN γ . **(e)** Quantitative PCR analysis of *Ifna* and *Ifnb* (n = 6 per group). **(f)** Secreted IFN β levels in the supernatants of MAECs. Left: stimulated for 3 h (n = 5 per group). Right: stimulated for 24 h (*Oasl1*^{+/+}: *p* = 0.0131, *Oasl1*^{-/-}: *p* = 0.0072, n = 6 per group). **(g)** Right: Western blot analysis of STAT1, STAT2, IRF7, and IRF3 expression. Left: Quantitation of band density. **b, c, e** and **g**, Box plots are shown as median of each value and the IQR; whiskers indicate 1.5 times the IQR. Data in **g** are representative of 3 independent experiments. Data are presented as means \pm SEMs (**p* \leq 0.05, ***p* \leq 0.01; **a–c**, two-sided unpaired Student's *t*-test; **e** and **f**, two-way ANOVA with Tukey's test; **g**, two-way ANOVA with Sidak's test for multiple comparisons). Source data are provided as a Source Data file.



Supplementary Figure 18. Endothelial *OASL* knockdown reduces *NOS3* levels and activates inflammation. **a** Quantitative PCR analysis of *Oasl1* and *Nos3* mRNA levels in MAECs isolated from *Oasl1*^{+/+} and *Oasl1*^{-/-} mice (*Oasl1*: $p = 0.0002$, *Nos3*: $p = 0.0009$, $n = 6$ per group). **b–c** HUVECs were transfected with non-targeting siRNA (siCTL) or *OASL*-targeting siRNA (siOASL). **(b)** *OASL* and *NOS3* mRNA levels as measured by quantitative PCR (*OASL*: $p = 0.0008$, *NOS3*: $p < 0.0001$, $n = 6$ per group). **(c)** Left: Immunocytochemical detection of eNOS. Scale bar, 20 μm . Right: Quantitation of corresponding MFI values ($p = 0.0031$, $n = 6$ per group). Scale bar, 20 μm . **d, e** Bulk RNA-seq analysis performed on siCTL- or siOASL-transfected HUVECs ($n = 2$ for each group). **(d)** Heatmap showing different gene expression patterns between two groups. **(e)** Gene ontology (GO) enrichment analysis of dysregulated biological processes in *OASL*-KD HUVECs. **f** MicroRNA (miRNA)-seq analysis performed on HUVECs transfected with siCTL or siOASL ($n = 2$ per group), depicted as a heatmap showing differences in miRNA expression patterns between the two groups. Data in **c** are representative of 6 independent experiments. Data are presented as means \pm SEMs (** $p \leq 0.01$, *** $p \leq 0.001$, **** $p \leq 0.0001$; **a–c**, two-sided unpaired Student's *t*-test; **e**, one-sided Fisher's exact test). Source data are provided as a Source Data file.



Supplementary Figure 19. Aortic endothelial OASL contributes to *NOS3* mRNA stability by regulating miR-584 levels. qRT-PCR analysis of miR-584 levels ($p < 0.0001$; $p = 0.0159$; $p = 0.0310$, $n = 4$ per group) (**a**) *NOS3* mRNA ($p = 0.0472$; $p = 0.0018$; $p = 0.0240$, $n = 4$ per group) (**b**) and *NOS3* mRNA stability in the presence of actinomycin D (AD; 3h NC vs. miR-584 mimic: $p = 0.0004$; NC mimic vs. inhibitor: $p = 0.0046$; miR-584 mimic vs. inhibitor: $p = 0.0059$; NC vs. miR-584 inhibitor: $p = 0.0473$, $n = 6$ per group) (**c**) in siCTL- or siOASL-transfected HUAECs, post-transfected with 80 nM negative control (NC) mimic, miR-584 mimic, NC inhibitor, or miR-584 inhibitor. NC: negative control. Data are presented as means \pm SEMs ($*p \leq 0.05$, $**p \leq 0.01$, $***p \leq 0.001$, $****p \leq 0.0001$; **a, b**, one-way ANOVA with Tukey's test; **c**, two-way ANOVA with Tukey's test for multiple comparisons). Source data are provided as a Source Data file.

Characteristics	<i>Apoe</i> ^{-/-}		<i>Oasl1</i> ^{-/-} <i>Apoe</i> ^{-/-}		<i>p</i> -value
	Mean	S.E.M.	Mean	S.E.M.	
Plasma glucose (mg/dl)	142.2	10.35	138.8	16.00	0.863
Triglyceride (mg/dl)	88.8	6.07	79.0	10.16	0.432
Total cholesterol (mg/dl)	620.8	21.05	591.2	22.82	0.368
HDL-C (mg/dl)	28.0	3.36	21.4	4.02	0.243
LDL-C (mg/dl)	120.6	8.57	129.2	14.16	0.617
ALB (g/dl)	4.0	0.05	3.8	0.14	0.188
GOT (IU/L)	248.0	13.56	254.0	31.40	0.865
GPT (IU/L)	148.0	20.83	116.0	9.80	0.202

Supplementary Table 1. Plasma lipid levels in *Oasl1*^{-/-}*Apoe*^{-/-} and *Apoe*^{-/-} mice. Plasma lipid profiles in *Oasl1*^{-/-}*Apoe*^{-/-} and *Apoe*^{-/-} mice fed a NCD for 28 weeks (n = 9 per group). Data are presented as means ± SEMs and analyzed using a two-sided unpaired Student's *t*-test.